

Christoph Hanhart^{1,2}, Daniel R. Phillips¹, and Sanjay Reddy²

¹*Department of Physics, University of Washington, Box 351560, Seattle, WA 98195-1560.*

²*Institute for Nuclear Theory, University of Washington, Box 351550, Seattle, WA 98195-1550.*

(March 31, 2000)

Neutrino and axion production in neutron stars occurs mainly as bremsstrahlung from nucleon-nucleon (NN) scattering. The energy radiated via neutrinos or axions is typically very small compared to other scales in the two-nucleon system. The rate of emission of such “soft” radiation is directly related to the on-shell NN amplitude, and thereby to the NN experimental data. This facilitates the model-independent calculation of the neutrino and axion radiation rates which is presented here. We find that the resultant rates are a factor of one half to one fifth below earlier estimates based on a one-pion-exchange NN amplitude.

Neutron stars are believed to be born during a supernova explosion with an interior temperature T of order 60 MeV. The subsequent evolution of the hot and dense compact star is characterized by a rapid early cooling phase followed by a, significantly slower, late-time cooling phase [1]. During both of these phases neutrinos are an important source of energy loss. Thermal evolution of neutron stars is largely driven by neutrino bremsstrahlung reactions such as

$$NN \rightarrow NN\nu\bar{\nu} \quad nn \rightarrow npe^-\bar{\nu}_e. \quad (1)$$

In the first part of the nascent neutron star’s life it evolves by diffusion of trapped neutrinos. This cools the interior to $T \sim 1$ MeV on a time scale of a few seconds [2]. The resultant intense neutrino emission is thought to play a central role in both the supernova mechanism and r-process nucleosynthesis. The high neutrino luminosity is fueled by the reactions (1), which compete with the annihilation $e^+ + e^- \rightarrow \nu\bar{\nu}$ in degenerate matter. At later times, the neutron star enters a period of slower thermal evolution, during which the emitted neutrinos free stream. This occurs because the neutrino mean-free path becomes long when $T \lesssim 1$ MeV. The time scale for this long-term cooling of the dense, degenerate, neutron-rich, inner core thus depends crucially on the neutrino emissivity, which is, again, dominated by the reactions (1). Observational constraints on this late-time portion of the neutron star’s evolution will improve as X-ray observatories such as Einstein, EXOSAT and ROSAT [1] gather pulsar data which gives information on the surface temperatures of these stars. The challenge for theorists is to improve the models of both the early- and late-time cooling of the neutron star.

The emissivities which are key ingredients in these simulations are dominated by the reactions (1). Despite their central role in neutron-star dynamics these reactions have received relatively little attention. The state of the art is still the pioneering work of Friman and Maxwell [3], where the reaction rates were computed using a nucleon-nucleon amplitude due only to a single pion exchange (henceforth we refer to this as the “OPE approximation”). Recently, many-body effects, in particular the suppression due to multiple scattering (the Landau-Pomeranchuk-Migdal, or LPM, effect [4]), have been shown to be important at temperatures $T \gtrsim 5$ MeV [5–8]. However, the treatment of the NN interactions which occur during the reactions (1) has not progressed beyond the OPE approximation. In this letter we follow an approach reminiscent of that used in soft-photon calculations [9], and relate the rate of production of soft-neutrino radiation in NN scattering to the on-shell NN scattering amplitude. This yields a calculation we present as a “benchmark”, which accounts for the two-nucleon dynamics in a model-independent way. We make no attempt to account for many-body effects, although they are undoubtedly important in the star. We identify the density and temperature range over which our results are valid and show that, although limited, it is of interest to both supernova and neutron star physics. In contrast, the full evaluation of the rates for the reactions (1) in a strongly-coupled medium is a complicated problem. Therefore, of necessity, most solutions to it will be model-dependent. Thus, we see our results as providing a model-independent foundation on which future work that assesses the role of many-body effects can build.

Our main focus in this work will be the neutrino emissivity from $NN \rightarrow NN\nu\bar{\nu}$. However, axions (if they exist) couple, like neutrinos, to the nucleon spin. Therefore, in computing the neutrino emissivity one obtains the axion emissivity from $NN \rightarrow NN a$ as a welcome by-product [6]. This is useful because one important constraint on the axion mass comes from considering the role of axionstrahlung in the dynamics of SN1987A [8,10]. Indeed, if the rate for the reaction $NN \rightarrow NN a$ is too high then the supernova dynamics is completely changed, and the successful “standard” picture of the supernova is destroyed. Thus, one can constrain the axion coupling, and hence the axion mass, by demanding that axion radiation did not make too large a contribution to the energy loss from SN1987A.

Neutrino and axion emissivities: We begin by explic-

itly calculating the emissivity due to $NN \rightarrow NN\nu\bar{\nu}$. The $\nu\bar{\nu}$ coupling to non-relativistic baryons at low energies is given by the Lagrange density

$$\mathcal{L}_W = -\frac{G_F}{2\sqrt{2}} l^\mu N^\dagger (c_v \delta_{\mu,0} - c_a \delta_{\mu,i} \sigma_i) N, \quad (2)$$

where $l^\mu = \bar{\nu} \gamma^\mu (1 - \gamma^5) \nu$ is the leptonic current, $G_F = 1.166 \times 10^{-5} \text{ GeV}^{-2}$, N is the nucleon field, and c_v and c_a are the nucleon neutral-current vector and axial-vector coupling constants. Some Feynman diagrams for the bremsstrahlung process are shown in Fig. 1.

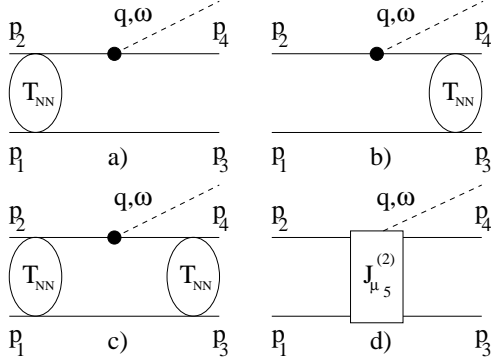


FIG. 1. Feynman diagrams for the bremsstrahlung process. The radiation is represented by the dashed line, and nucleons by solid lines. T_{NN} is the NN transition matrix and $J_{\mu 5}^{(2)}$ is a two-body axial current.

The incoming (outgoing) nucleon momenta are labeled $\mathbf{p}_1, \mathbf{p}_2$ ($\mathbf{p}_3, \mathbf{p}_4$). The dashed line represents radiation—a neutrino-anti-neutrino pair in this case—which carries energy ω and momentum \mathbf{q} . In general we are interested in cases where the radiated energy is small compared to the incoming nucleon energy. In the limit $\omega \rightarrow 0$ the amplitudes corresponding to diagrams (a) and (b) in Fig. 1 are dominant, as they contain pieces proportional to $1/\omega$. On the other hand, the contributions from the rescattering diagram Fig. 1(c), and from meson-exchange currents such as Fig. 1(d), remain finite in the $\omega \rightarrow 0$ limit. Thus, for the reaction $nn \rightarrow nn\nu\bar{\nu}$ the matrix element can be written as

$$\mathcal{M} = 2 \frac{G_F}{2\sqrt{2}} \frac{1}{\omega} l^\mu \langle \mathbf{p}' | [T_{NN}, \Gamma_\mu] | \mathbf{p} \rangle + O(\omega^0), \quad (3)$$

where $\mathbf{p}(\mathbf{p}')$ is the initial (final) relative momentum of the two-nucleon system. We refer to results which retain only this leading term, of $O(\omega^{-1})$, in \mathcal{M} as “true in the soft-neutrino approximation (SNA)”. In general the NN T-matrix appearing in Eq. (3), T_{NN} , will be half off-shell¹. But, in the SNA we can take T_{NN} to be the on-

shell NN amplitude. We can also neglect the difference between the magnitude of the initial and final-state relative momenta. We expect these approximations to break down when $\omega \sim m_\pi$, since m_π sets the scale for variations of T_{NN} in the off-shell direction². So, in the SNA, the NN interaction is described by the on-shell T-matrix T_{NN} , evaluated at a center-of-mass energy which, for reasons of symmetry, is chosen to be $(p^2 + p'^2)/(2M)$ (M is the nucleon mass). This T-matrix can be constructed from phase shifts deduced from NN scattering data [11]. Note that the OPE approximation used in most previous calculations involves substituting V_{OPE} , the one-pion-exchange *potential*, for T_{NN} in Eq. (3). Meanwhile, Γ_μ is the vertex which couples the radiation to the nucleons. For $\nu\bar{\nu}$ radiation Γ_μ follows straight from Eq. (2). Only its three-vector part contributes to \mathcal{M} at $O(\omega^{-1})$. Equation (3) then gives us a model-independent result for \mathcal{M} , which is correct in the SNA.

If only two-body collisions are taken into account then the neutrino emissivity from a neutron gas is given by Fermi’s golden rule

$$\mathcal{E}_{\nu\bar{\nu}} = \int \frac{d^3 q_1}{(2\pi)^3 2\omega_1} \frac{d^3 q_2}{(2\pi)^3 2\omega_2} (2\pi)^4 \delta(E_{in} - E_{fn}) \omega \delta^3(\mathbf{p}_{in} - \mathbf{p}_{fn}) \int \left[\prod_{i=1..4} \frac{d^3 p_i}{(2\pi)^3} \right] \mathcal{F} \frac{1}{s} \sum_{\text{spin}} |\mathcal{M}|^2, \quad (4)$$

where $\mathcal{F} = f_1 f_2 (1 - f_3) (1 - f_4)$, with $f_i = 1/(1 + \exp(E_i - \mu_i)/T)$ being the Fermi-Dirac distribution function for the nucleons, and $s = 4$ the symmetry factor accounting for identical nucleons. The spin-summed square of the matrix element can be factored into leptonic and hadronic tensors, and then represented by

$$\sum_{\text{spin}} |\mathcal{M}|^2 = \frac{G_F^2 c_a^2}{8} \text{Tr} (l^i l^j) \mathcal{H}_{i,j}. \quad (5)$$

The trace over the lepton tensor is easily evaluated. Further, since we are interested in soft radiation, we may safely ignore \vec{q} in the momentum delta function [3]. This allows us to directly integrate the leptonic trace over neutrino angles to obtain

$$\int d\Omega_1 \int d\Omega_2 \text{Tr} (l^i l^j) = 8 (4\pi)^2 \omega_1 \omega_2 \delta_{i,j}. \quad (6)$$

Therefore, only the trace of the hadronic tensor \mathcal{H}_{ij} contributes to the emissivity, and so we define a scalar function,

¹As used here, it should involve a sum over the allowed partial-waves of the NN system. This, together with the factor of two in front of the matrix element, accounts for the exchange graphs which must be included in \mathcal{M} .

²At very low relative momenta the scale of breakdown is set by the NN scattering length, since that gives the variation in the on-shell direction. However, a_{NN} does not really play a role here, since typical nucleon momenta in neutron stars are at least 100 MeV.

$$S_\sigma(\omega) = \int \left[\prod_{i=1..4} \frac{d^3 p_i}{(2\pi)^3} \right] (2\pi)^4 \delta^3(\mathbf{p}_1 + \mathbf{p}_2 - \mathbf{p}_3 - \mathbf{p}_4) \delta(E_1 + E_2 - E_3 - E_4 - \omega) \mathcal{F} \frac{1}{s} \mathcal{H}_{ii}, \quad (7)$$

which is called the dynamical spin structure function of the medium. It is related to the $\nu\bar{\nu}$ emissivity via:

$$\mathcal{E}_{\nu\bar{\nu}} = \frac{G_F^2 c_a^2}{16\pi^4} \frac{1}{30} \int d\omega \omega^6 S_\sigma(\omega), \quad (8)$$

where ω is the total energy of the emitted $\nu\bar{\nu}$ pair.

In the two-body approximation considered here we evaluate \mathcal{H}_{ii} using Eqs. (3) and (5). For the case of emission from the nn system, only the spin-triplet two-nucleon state contributes, and the trace is:

$$\mathcal{H}_{ii} = 16 \frac{1}{\omega^2} \sum_{M_s M'_s} |\langle 1M'_s, \mathbf{p}' | [S_i, \mathbf{T}_{NN}] | \mathbf{p}, 1M_s \rangle|^2, \quad (9)$$

where S_i is the total spin of the two-nucleon system. It is straightforward to generalize this formula for \mathcal{H}_{ii} to the np case, although there the NN spin singlet also plays a role. From Eqs. (9) and (7) we can calculate S_σ , and thus the $\nu\bar{\nu}$ emissivity.

The emission of any radiation which couples to the nucleon spin will be described by the same function S_σ . Thus, as mentioned above, with S_σ in hand we may derive the axion emissivity \mathcal{E}_a . The effective theory for axion-nucleon interactions is described by the Lagrange density $\mathcal{L}_{\text{ann}} = -g_{\text{ann}} a \bar{N} \gamma^5 N$, where a is the axion field, and $g_{\text{ann}} = 10^{-8} (m_a/1 \text{ eV})$ is the effective axion coupling (m_a is the axion mass) [12]. The calculation of the axion emissivity in this effective theory is analogous to the above calculation of the neutrino emissivity, and yields

$$\mathcal{E}_a = \frac{g_{\text{ann}}^2}{16\pi^2 M^2} \frac{1}{3} \int d\omega \omega^4 S_\sigma(\omega). \quad (10)$$

Before proceeding to our results we note that S_σ can be defined in a much more general way, where it describes the response of a many-body system to an external spin-dependent perturbation. Equations (8) and (10) remain true if this definition is adopted. To obtain Eq. (7) for S_σ in this general case one takes the long-wavelength limit of the leading term in the density expansion.

Results & Discussion: We present results for the dynamic spin structure function $S_\sigma(\omega)$, since it includes the density, temperature, and nuclear dynamics dependence of the neutrino and axion emissivities. During the evolution of neutron stars, one encounters varying degrees of nucleon degeneracy, with $\mu_n/T \sim 1$ at birth, but $\mu_n/T \gg 10$ at late times. Earlier investigations have shown that analytic approximations to the phase-space integrals in Eq. (7) work poorly at intermediate degeneracy [10]. Therefore, in this work these integrals are all performed numerically. In order to investigate the

effect of our model-independent treatment of the NN interaction we plot the ratio $R_\sigma(\omega) \equiv S_\sigma^{SNA}(\omega)/S_\sigma^{\text{ref}}(\omega)$, where $S_\sigma^{SNA}(\omega)$ is calculated as described above. The denominator, $S_\sigma^{\text{ref}}(\omega)$, is the dynamic spin structure function found when a hadronic tensor trace of the form $\mathcal{H}_{ii} = c/\omega^2$ is inserted into Eq. (7). We adjust the constant c so that when S_σ^{ref} is employed in Eq. (8) the neutrino emissivity thereby obtained is equal to that found if the *full* OPE matrix element is used in evaluating \mathcal{H}_{ii} ³.

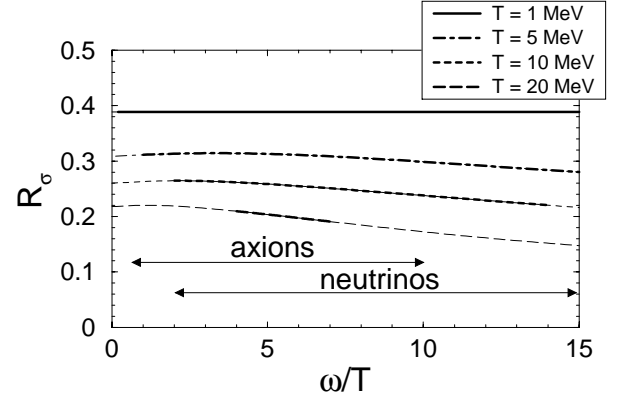


FIG. 2. A plot showing the ratio $R_\sigma = S_\sigma^{SNA}/S_\sigma^{\text{ref}}$ for nn pairs in neutron matter at a density of 0.16 fm^{-3} . The region where multiple scattering suppression due to the LPM effect is negligible ($\omega > \gamma$, see below), and the SNA is expected to be valid ($\omega < m_\pi$) is delineated by thicker curves. The regions probed by the neutrino and axion emissivities are different, as indicated on the plot.

Figure 2 shows the resulting ratio $R_\sigma(\omega)$ for neutron matter at a range of temperatures and a baryon density equal to the nuclear saturation density. The results are plotted as a function of the dimensionless ratio ω/T (note $S_\sigma(\omega)$ has significant strength only for $\omega/T \lesssim 15$).

The most striking feature of the results is that the one-pion-exchange approximation significantly overestimates the rate for neutrino (or axion) production. The large reduction in the response functions over those obtained in the OPE approximation occurs for two reasons. Firstly, one-pion exchange over-estimates the strength of the NN tensor force, and so even replacing the V_{OPE} employed previously with the full V_{NN} would lead to a reduction in S_σ . Secondly, and more importantly, the unitarity of our NN T-matrix leads to an NN amplitude which is, in general, significantly smaller than that found in the OPE approximation, and hence to a much-reduced S_σ .

³We could have followed Refs. [8,10] and adopted a reference $S_\sigma(\omega)$ in which the full OPE-approximation matrix element is replaced by its value in the $m_\pi \rightarrow 0$ limit. However, this is a poor approximation to the actual result for one-pion exchange, since it over-estimates the OPE-approximation emissivities by as much as a factor of two (see also Refs. [6,10]).

Further, Fig. 2 allows us to infer where the SNA breaks down. Recall that S^{ref} is constructed using a hadronic tensor \mathcal{H}_{ij} proportional to $1/\omega^2$. In fact this part of the hadronic response is the only piece of the \mathcal{H}_{ij} calculated in the SNA that can be trusted. Therefore, any ω -dependence of $R_\sigma(\omega)$ represents an effect in $S_\sigma^{\text{SNA}}(\omega)$ coming from physics beyond the SNA. Viewing Fig. 2 in this light, and considering the constraint $\omega \lesssim m_\pi$, implies that at $\rho = \rho_0$ the SNA works well for $T \lesssim 10$ MeV.

The suppression of the axial response seen in Fig. 2 translates into a corresponding diminution of axion and neutrino emissivities. Let us define the ratio $R_{\mathcal{E}_\nu} \equiv \mathcal{E}_{\nu\bar{\nu}}^{\text{SNA}}/\mathcal{E}_{\nu\bar{\nu}}^{\text{OPE}}$. Here, $\mathcal{E}_{\nu\bar{\nu}}^{\text{OPE}}$ is the emissivity found in the OPE approximation, as calculated in Ref. [3]. (A similar ratio of axion emissivities is approximately equal to $R_{\mathcal{E}_\nu}$ in the domain of validity of the SNA.) The ratio $R_{\mathcal{E}_\nu}$ is displayed in the table below for a range of densities and at temperatures of 1 and 10 MeV. In fact, the temperature and density dependence of $\mathcal{E}_{\nu\bar{\nu}}^{\text{SNA}}$ is predominantly determined by that of the nucleon equilibrium distribution functions appearing in Eq. (4), but the ratio $R_{\mathcal{E}_\nu}$ changes significantly over the densities and temperatures considered because $\mathcal{E}_{\nu\bar{\nu}}^{\text{OPE}}$ has much more variation with n_B and T . We see that, for the range of conditions considered here, the SNA gives a rate of emission of soft axial radiation which is a factor of two to five smaller than that given by the OPE approximation.

| n_B (fm $^{-3}$) | $R_{\mathcal{E}_\nu}^{nn}$ (1 MeV) | $R_{\mathcal{E}_\nu}^{nn}$ (10 MeV) |
|---------------------|------------------------------------|-------------------------------------|
| 0.08 | 0.46 | 0.28 |
| 0.16 | 0.38 | 0.25 |
| 0.48 | 0.24 | 0.19 |

Disclaimers: As mentioned previously, our calculation makes no attempt to include many-body effects. These will certainly be important in some regimes of temperature and density. For instance, it is claimed that in-medium modifications of the pion, attributed to the many-body nature of the problem, strongly affect the emission rates [13]. Such effects are outside the scope of this work. However, as stated earlier, we expect the LPM effect to strongly reduce the response function [5–8]. In particular, it will suppress the emission of radiation with $\omega \lesssim \gamma$, where γ is the nucleon quasi-particle width at the Fermi surface. This LPM-effect limit on the validity of our calculation is indicated in Fig. 2, with the value of γ taken from Ref. [7]. Figure 2 suggests that LPM-suppression will affect the emissivity if $T > 10$ MeV. Note that the LPM effect and the use of the SNA *both* significantly reduce the rate of emission of soft axial radiation.

Several microphysical ingredients play a role in the thermal evolution of neutron stars, and so it is difficult to state precisely how the results obtained in this work will affect observable aspects of neutron star evolution. However, our results imply that NN bremsstrahlung is less important during the star’s infancy than previously

thought. In addition, the reduction of the axion emissivity we have found will, presumably, weaken the axion-mass bound obtained from SN1987A. However, these comments are subject to the caveat that through large regions of the infant neutron star the temperature is high enough to invalidate the SNA.

On the other hand, for late-time cooling the temperature is small, and our results are applicable everywhere in the star. However, in this regime the modified URCA reaction, $nn \rightarrow npe^- \bar{\nu}_e$, is significantly more efficient than the pair process considered here [3]. In degenerate matter this charged-current reaction does not produce soft radiation, since the typical change in the energy of the NN system is of order the electron chemical potential, i.e. about 100 MeV. Nevertheless, the results presented here suggest that large corrections to the modified URCA rate calculated in the OPE approximation will occur when a better model of the NN amplitude is used.

Conclusion: Finally, we reiterate that none of these disclaimers modify the two central conclusions of this paper: that the soft-neutrino approximation gives a model-independent result for the emissivity due to the reactions $NN \rightarrow NN\nu\bar{\nu}$ and $NN \rightarrow NN\pi$; and that these emissivities are much smaller than those found when one-pion exchange is used as the NN amplitude.

Acknowledgements: We are grateful to J.-W. Chen and M. J. Savage for useful discussions. We thank the U. S. Department of Energy for its support under contracts DOE/DE-FG03-97ER4014 and DOE/DE-FG06-90ER40561. C. H. acknowledges the support of the Alexander von Humboldt foundation.

-
- [1] S. Tsuruta, Phys. Rep. **292**, 1 (1998).
 - [2] A. Burrows, Ann. Rev. Nucl. Part. Sci. **40**, 181 (1990).
 - [3] B. L. Friman and O. V. Maxwell, Ap. J. **232**, 541 (1979).
 - [4] L. D. Landau and I. Ya. Pomeranchuk, Dokl. Akad. Nauk Ser. Fiz. **92**, 735 (1953); A. B. Migdal, Phys. Rev. **103**, 1811 (1956).
 - [5] J. Knoll and D. N. Voskresensky, Ann. Phys. (N.Y.) **249**, 532 (1996).
 - [6] G. Raffelt and D. Seckel, Phys. Rev. **D52**, 1780 (1995).
 - [7] A. Sedrakian and A. Dieperink, Phys. Lett. **B463**, 145 (1999); astro-ph/0002228.
 - [8] W. Keil, H.-T. Janka, D. N. Schramm, G. Sigl, M. S. Turner, and J. Ellis, Phys. Rev. **D56**, 2419 (1997).
 - [9] F. E. Low, Phys. Rev. **110**, 974 (1958).
 - [10] R. P. Brinkmann and M. S. Turner, Phys. Rev. **D38**, 2338 (1988).
 - [11] Extracted from the SAID partial-wave analysis facility (<http://said.phys.vt.edu/>).
 - [12] D. B. Kaplan, Nucl. Phys. **B260**, 215 (1985).
 - [13] D. N. Voskresensky and A. V. Senatorov, Sov. J. Nucl. Phys. **45**, 411 (1987).